

Photochemical & Photobiological Sciences

Accepted Manuscript



This is an *Accepted Manuscript*, which has been through the Royal Society of Chemistry peer review process and has been accepted for publication.

Accepted Manuscripts are published online shortly after acceptance, before technical editing, formatting and proof reading. Using this free service, authors can make their results available to the community, in citable form, before we publish the edited article. We will replace this *Accepted Manuscript* with the edited and formatted *Advance Article* as soon as it is available.

You can find more information about *Accepted Manuscripts* in the [Information for Authors](#).

Please note that technical editing may introduce minor changes to the text and/or graphics, which may alter content. The journal's standard [Terms & Conditions](#) and the [Ethical guidelines](#) still apply. In no event shall the Royal Society of Chemistry be held responsible for any errors or omissions in this *Accepted Manuscript* or any consequences arising from the use of any information it contains.

1 From Ultraviolet to Prussian blue: A spectral response for the cyanotype process and a safe
2 educational activity to explain UV exposure for all ages.

3 Turner, J¹, Parisi, AV¹, Downs, N¹ and Lynch, M¹

4 ¹University of Southern Queensland, Toowoomba. Australia.

5

6 Abstract

7 Engaging students and the public in understanding UV radiation and its effects is achievable using the
8 real time experiment that incorporates blueprint paper, an “educational toy” that is a safe and easy
9 demonstration of the cyanotype chemical process. The cyanotype process works through the presence
10 of UV radiation. The blueprint paper was investigated to be used as not only engagement in
11 discussion for public outreach about UV radiation, but also as a practical way to introduce the
12 exploration of measurement of UV radiation exposure and as a consequence, digital image analysis.
13 Tests of print methods and experiments, dose response, spectral response and dark response were
14 investigated. Two methods of image analysis for dose response calculation are provided using easy to
15 access software and two methods of pixel count analysis were used to determine spectral response
16 characteristics. Variation in manufacture of the blueprint paper product indicates some variance
17 between measurements. Most importantly, as a result of this investigation, a preliminary spectral
18 response range for the radiation required to produce the cyanotype reaction is presented here, which
19 has until now been unknown.

20

21 Keywords: ultraviolet radiation, Prussian blue, cyanotype, educational activity, UV, spectral response.

22

23 1.0 Introduction

24 Improving public understanding of ultraviolet (UV) radiation and how it impacts human health (both
25 beneficial and hazardous implications) is an ongoing challenge that constantly needs reinforcement
26 from research institutions to the public [1]. This is a topical problem especially for countries like
27 Australia which experiences the highest incidence rates of skin cancer in the world [2]. Due to the
28 time lag between UV exposure and skin cancer development, it is difficult to provide definitive
29 evidence to the public of the connection. However many studies are working to close that gap [3, 4]
30 especially with the impact of the diminished ozone layer [5, 6] and its predicted slow recovery [7]. In
31 general, it is accepted that UV radiation causes skin cancer as endorsed by the World Health
32 Organisation [8]. Despite the established knowledge base connecting UV radiation and skin cancer
33 [3-5, 9], there is still public misunderstanding which can be damaging to the beneficial effects of
34 public health campaigns [10, 11].

35 One of the key factors that assist in promoting sun protection campaigns in skin cancer prevention is
36 the education of children and the public. A review of studies by Stanton et al [12] indicates children
37 were reported to depend on parents' sun protective behaviour. Primary schools are also shown to be
38 effective in moderating sun exposure behaviour [13]. Therefore education of both children and adult
39 populations are equally important in sun protection education. One of the most difficult issues in
40 demonstrating the effects of UV radiation is being able to show a physical effect in real time
41 specifically due to UV radiation before the onset of erythema. UV radiation is not sensed like thermal
42 radiation (although there is evidence to indicate that the two are regularly confused by the public
43 [10]), and thermal comfort does indirectly affect behaviour in an UV environment [14, 15]. The
44 biological effects due to UV radiation are delayed in relation to original exposure periods, which may
45 contribute to lack of public understanding. Skin cancer results from a number of factors over years of
46 exposure [3-5, 9]. Even short term human biological responses, such as erythema (sunburn) [16] and
47 photokeratitis (also known as snowblindness) [17] occur after a period of hours, due to excessive UV
48 exposure. A mechanism to allow the public and children to immediately understand the connection
49 between exposure and deleterious health effects is required. The notable latency between exposure
50 and biological effect are not appropriate for educational purposes.

51 There is a commercially available simple "educational toy", which will be called blueprint paper
52 hereafter that can be employed to demonstrate an immediate physical response to UV radiation in real
53 time that can be observed easily and safely by anyone. The product is not new, and has been readily
54 available from scientific educational stores for many years, but has never been effectively studied for
55 its response to the biologically weighted UV spectrum. This article aims to analyse blueprint paper so
56 that UV researchers and educators can be confident of its effectiveness in responding to UV radiation,
57 and, therefore can be used as a "hands-on" engagement activity for students and the public alike.

58 Education research shows that “hands-on” activities promote greater understanding than any other
59 form of learning.

60 The blueprint paper is a solar radiation sensitive paper. The paper is based on the principle of
61 cyanotype, an alternative to the early forms of silver based photographic printing that was published
62 by John Hershel in 1842 as a post-script [18] and was subsequently used as the method of producing
63 blueprints for designs and schematics in the 20th century. History and information regarding the
64 technique of cyanotyping has been extensively documented [19]. The chemical process of producing
65 the colour Prussian blue in the cyanotype has also been documented [20]. Prussian blue is the product
66 of the reaction between either iron (III) and ferrocyanide ions, or iron (II) and ferricyanide ions. Iron
67 (II) ions are generated by the photochemical decomposition of iron (III) complexes with ligands such
68 as oxalate or citrate, through a photo-activated redox reaction. The iron (II) ions are then free to react
69 with ferricyanide to produce Prussian blue. The photo-activation in the cyanotype process occurs most
70 easily due to ultraviolet and extreme violet radiation exposure [21]. Prussian blue is an insoluble
71 product, but can be embedded in paper or cloth when the chemical process takes place. This is a
72 common experiment for undergraduate students undertaking chemistry, by soaking cloth in the
73 prepared reactants before exposing the cloth and adding an overlying negative type image, to solar
74 radiation to initiate the cyanotype process. This procedure is called the “printing-out-process” since it
75 does not require any other development to produce the image [22]. Any unreacted salts can be washed
76 from the cloth leaving an image of the negative in shades of blue. Recently this technique has been
77 used to create a simple solar radiation dosimeter, with depth of Prussian blue colouring in the cloth
78 correlated to solar UV exposure [23].

79 The blueprint paper (of varying sizes depending on manufacturer) has embedded reactants that
80 undergo the above reaction when exposed to solar radiation. The blueprint paper is provided as a dry
81 product, and during exposure shows pale blue fading to greenish-white. After exposure the paper is
82 rinsed in water to remove unreacted salts. During the rinse process, it can be observed that the white
83 areas will change to blue within just a minute of rinsing. After drying, the paper shows deep blue
84 where sunlight caused a reaction and white (no exposure) to shades of blue (low to medium exposure)
85 depending on level of exposure to solar radiation. This inverse of the colours during exposure and
86 development have been used to simulate film photography methods [24]. Given the simplicity of the
87 blueprint paper development, in that it does not require a wet lab for the experiment (only access to
88 water), and can be safely used by children and adults of all ages, it was hypothesised that the
89 applications seen by the cloth experiment in UV exposure measurement could be reproduced using
90 the blueprint paper.

91 UV radiation and visible light are assigned the role of the sensitiser in the blueprint paper just like that
92 of the cyanotype process. However, there appears to be little documented evidence as to exactly what

93 part of the solar spectral range is the primary initiator of the reaction. Work done by Price et al. [25]
94 used blueprint paper to study light distribution on grape clusters. Blueprint paper was used in place of
95 ozalid paper, a photosensitive paper used to observe light distribution in ecological and plant based
96 studies [26] that required development in a chamber with ammonia gas [25]. However, Price et al
97 reported they could not obtain a spectral response of the blueprint paper from the manufacturer and
98 that lack of a spectral response would limit the use of the blueprint paper in their devised experimental
99 method. Price et al. assumed that blueprint paper must be most responsive in the violet and ultraviolet
100 spectrum (similar to ozalid paper), based on unpublished data that reported the paper having no
101 response to wavelengths above 500 nm. Ware [21] stipulates that maximum effect is observed due to
102 the near ultraviolet and blue light spectra, although he also states that this range is 300 nm to 400nm
103 and known as UVA radiation. A breakdown of the UV spectrum consists of UVC radiation (200 nm
104 to 280 nm), UVB radiation (280 nm to 315 nm) and UVA radiation (315 nm to 400 nm) [27, 28] and
105 above 400 nm as violet or visible radiation (the division between UVA and UVB may also be stated
106 in some sources at 320 nm for other areas of study [29, 30]). For solar UV studies those divisions are
107 limited to UVB (290 nm to 315 nm) since there is no terrestrial UVB below 290 nm, UVA (315 nm to
108 400 nm) and visible (400 nm and above). However, lack of consistent nomenclature notwithstanding,
109 there is evidence to indicate UV radiation is the main initiator of this reaction despite a lack of
110 published work in this regard. This study will characterise the blueprint paper, by providing a dose
111 response and a preliminary spectral response for the cyanotype process that produces the dye Prussian
112 blue. These qualities will provide the certainty that blueprint paper can be used to demonstrate effects
113 due to UV radiation to the public and students. Example demonstration uses will also be provided.

114

115 2.0 Methodology

116 Blueprint paper is available commercially through three companies of manufacture, with each
117 blueprint paper marketed with different names. These companies, the product name and the company
118 website are listed in Table 1. At least two of the three companies export their products with Australian
119 suppliers listed (from which the product was obtained). Samples of the blueprint paper were
120 purchased from the companies and two of the three tested in this study. The third blueprint paper was
121 not tested due to its discovery of production after all of the tests were completed. A legend for each
122 commercial product used in the following study is provided in Table 1, in which each company of
123 manufacture is referred to as Paper 1, 2 or 3. Lawrence and Fishelson [22] also provide instruction on
124 creating one's own version of this paper.

125 2.1 Spectral Response

126 Paper 1 was divided into smaller sized sheets and individually exposed to UV radiation. The paper
127 was cut to sizes of 3 cm × 4 cm and was held in place using a film transparency holder measuring 3.5
128 cm × 2.3 cm. The UV radiation was produced by an irradiation monochromator with a 1600 W lamp
129 (model 66390 Oriel Instruments, California, USA) and double grating monochromator (model 74125
130 Oriel Instruments, California, USA) controlled by a digital exposure controller (model 68591, Oriel
131 Instruments, California, USA). Input and output slits were set to 4.5 mm and 4.0 mm respectively.
132 The output beam covered the film transparency aperture. Each sheet of blueprint paper segment was
133 exposed to 2000 J/m² per 10 nm step with an average full-width-half-maximum (FWHM) of 5.2 nm,
134 starting at 280 nm to 430 nm in the initial test run. Following tests increased this range to 450 nm.
135 The blueprint paper was placed at 16.4 cm from the irradiation monochromator aperture. The
136 exposure was calculated by measuring the output of the irradiation monochromators using a
137 spectroradiometer (model DMc150, Bentham Instruments Ltd, Reading UK) and calculating the
138 equivalent time for exposure. The minimum exposure for a response of the chemical process is 34
139 J/m² [21]. The dose of 2000 J/m² for each exposure per wavelength was used after a number of trials
140 at a variety of exposure amounts and times. Exposure ranges from 500 J/m² to 1500 J/m² did not
141 provide information that would withstand the pixel counting procedure (producing low to no counts
142 compared to a saturated exposed reference sheet), and exposures well above 2000 J/m² often saturated
143 the paper. Consequently, the exposure of 2,000 J/m² provided the most appropriate indication per
144 wavelength of radiant UV sensitivity. Examples of a “no exposure” and “saturated exposure”
145 reference sheet are provided in Figure 1 for both Paper 1 and Paper 2. It is interesting to note that the
146 saturation is deeper in Paper 2 than Paper 1. Saturation was achieved using the full solar spectrum.
147 Paper 1 also shows that the protective layer that covered the “no exposure” side was moved during
148 exposure, leaving a mid-tone exposure in the centre of the sheet. This central section of the image was
149 not used as part of the reference sheet (detailed next). After exposure each blueprint paper sheet was
150 washed in water, dried and photographed using a digital camera Nikon D7000 with 18-105 mm lens.
151 To ensure no variation between photographs, each paper sheet was photographed on an illuminated
152 white background, using the set photographic controls including a pre-set white balance for the
153 illuminated background (daylight with additional lamp lighting) without any other objects on the page
154 (as compared to an 18% grey card which provides colour balance between neutral colours in an
155 image, and helps to prevent under- or over-exposure of an image). The manual settings of the camera
156 included an aperture of f/9, shutter speed of 1/50, ISO of 800 with no flash. The focal length of the
157 camera is recorded at 32 mm with a 35 mm lens focal length at 48 mm. The images of each exposed
158 piece of paper were then cropped to the same dimensions to show blue print paper only. Two methods
159 of pixel counting were used to determine effect of exposure per wavelength. An algorithm developed
160 to count blue pixels in a sky image used in Downs, et al. [31] was used to count the number of dark
161 blue pixels as stipulated by a saturation amount. The second method was the use of the program
162 Multispec (for Windows) which is used for analysis of multispectral image data. Each method

163 requires that a reference sheet of the same paper type must have two controls, with a sample of
164 unexposed blueprint paper and fully saturated blueprint paper, with the same photographic treatment
165 as the spectrally treated paper (dimension size is less important). For each method the reference sheet
166 is used in a slightly different manner as described below.

167 2.1.1 Blue sky algorithm image analysis

168 The reference sheet was used to determine if the blue pixel counting algorithm is set at an appropriate
169 saturation level. Blue pixels set above the saturation level will be counted as blue sky (or exposed
170 paper) whereas blue pixels set below the saturation level will not be counted (and considered as
171 unexposed paper). This provides a quantitative, consistent method of counting saturation level. Each
172 image taken for the spectral response is analysed using the algorithm, and a processed image can be
173 produced indicating areas of exposed and unexposed pixels. The reference sheet when set at an
174 appropriate saturation level will show no speckling of pixels in either the exposed or unexposed
175 sections after being processed by the algorithm.

176 2.1.2 Multispec image analysis

177 The reference sheet using this image analysis software is used differently to the blue sky algorithm, in
178 that it sets the level of saturation prior to image analysis. Multispec software is freely available at
179 <https://engineering.purdue.edu/~biehl/MultiSpec/> for both Mac and PC and provides instructions for
180 use. Training fields are selected in the areas of exposed and unexposed areas of the blueprint paper
181 image. Using the pixel information obtained in this reference image (it is easiest to use an image that
182 has both clearly defined exposed and unexposed sections), the spectral response blueprint paper
183 images can then be analysed using the classify function. Processed images of the counted pixels can
184 also be produced to visualise the counts of exposed to unexposed pixels.

185 For each method of analysis, the total percentage of pixel counts per image for exposed pixels is
186 calculated. The image with the highest percentage pixel count is allocated a maximum value of 1.0
187 and the remaining percentage pixel counts in the same data set are adjusted using this ratio. The
188 normalised pixel count is then plotted against wavelength of exposure to produce the spectral
189 response.

190 2.2 Dose response

191 Using the study by [23] as a guide, simple tests of dose response were investigated for the blueprint
192 paper. The test is the same as a photographic film development, where sections of the paper are
193 exposed for increasing periods of time to radiation to determine the optimum exposure time for an
194 image. Initial investigations revealed that blueprint paper has an extremely fast reaction time, with full
195 saturation of the paper (producing the characteristic deep blue result of Prussian blue after washing

196 and drying) in less than one minute exposure on a sunny winter's day in Toowoomba (27.5° S, 151.9°
197 E) at noon (44.9° SZA). Ware [21] identified that the cyanotype reaction only requires a very low
198 radiant energy density of 34 J/m² to produce a perceptible visual effect. Further tests of shorter time
199 intervals were made, that indicated intervals of 10 seconds, whilst providing a visible indication that a
200 dose response is apparent, is still too fast for effective scientific investigations about exposure times.
201 A neutral density filter consisting of thin white plastic (household garbage bags) was used to slow the
202 dose response. Transmission tests using a spectrophotometer (UV-2700, Shimadzu & Co, Kyoto,
203 Japan) indicate that a single layer of the neutral density filter has an average spectral transmission
204 from 280 nm to 400 nm of 8.5% and from 400 nm to 700 nm an average of 12%. A double layer of
205 neutral density filter was shown to have an average transmission of 2.3% for the range of 280 nm to
206 400 nm and 3.8% transmission for 400 nm to 700 nm. The overall transmission values are provided in
207 Figure 2 [32].

208 The dose response of Paper 2 (see Table 1) was tested on September 7, 2013 on a sunny day (51 to
209 56.7° SZA), using each (single and double) neutral density filter layer. To create the paper dose
210 response, one sheet of blueprint paper (10 cm × 10 cm) was divided into smaller pieces (2 cm × 2 cm
211 square) to limit sheet variation and batch variation per paper type. Two controls were created per dose
212 response. One piece was not exposed to any solar UV irradiance, whilst a second was exposed to solar
213 UV irradiance for several minutes to obtain saturation. Under one layer of the neutral density filter,
214 ten pieces of blueprint paper were exposed to solar UV irradiance in time intervals of 30 seconds,
215 whilst the solar UVB exposure was measured concurrently. An additional dose response using two
216 layers of neutral density filter with increasing intervals of 1 minute exposure to solar UV irradiance
217 was carried out with measured solar UVB exposure.

218 A broadband UVB sensor (IL-1400, International Light Inc, Massachusetts, USA) was used to
219 measure the UV radiation exposure for the transmitted UV radiation with the corresponding layers
220 neutral density filter (one layer for a five minute dose response and a double layer for a ten minute
221 dose response) over the sensor. The neutral density filter was stretched as taut as possible across both
222 the blueprint paper and the UVB detector head during each dose response measurement. The sensor
223 (model SEL240, International Light Inc) is used with a UVB Detector Head with a wavelength
224 sensitivity range from 256 nm to 314 nm. This instrument is regularly calibrated against a scanning
225 spectroradiometer (model DTM 300, Bentham Instruments, Reading, UK) located on a nearby
226 building rooftop, and therefore it is possible to correlate the UVB measured to the entire UV
227 spectrum. The ambient UV exposure was calculated from the UV irradiances recorded by the
228 spectroradiometer. The spectroradiometer is kept temperature stabilised in an environmentally sealed
229 box at 25.0° ± 0.5°. The spectroradiometer runs continuously from 5.00 am to 7.00 pm and makes
230 global and diffuse scans alternating throughout the day so that global scans are carried out on the 0,
231 10, 20, 30, 40, and 50 minute interval in the hour and the diffuse scans are carried out on the 5, 15, 25,

232 35, 45 and 55 minute interval in the hour. Each dose response measurement was carried out mid-
233 afternoon 7 September 2013. The corresponding afternoon group of global scans from the
234 spectroradiometer were collated (from 2.00 pm to 3.30 pm). The spectral UV erythemal irradiance
235 was collected, the exposure values calculated and plotted against time in order to obtain a polynomial
236 line of best fit. Using the line of best fit, ambient UV exposure values were calculated at the times the
237 measurements were taken and then cumulatively combined per increase in time.

238 After exposure each piece of blueprint paper was washed in water, dried and photographed. The
239 camera settings were the same as those used for the spectral response using the same set up and
240 background, except the camera focal length is recorded at 34mm with the lens 35mm focal length at
241 51 mm. As these are analysed separately to the dose response images, a slight variation in distance is
242 negligible. Given the size of the blueprint paper pieces, all pieces in a dose response set fitted into
243 one photograph, thus limiting any further variation between images. Each section of blueprint paper
244 was then cropped from the image using Photoshop CS6 with no white background present in each
245 individual timed dose with the same dimensions per cropped image. Information about each timed
246 dose or control piece was obtained either using Photoshop or a method devised by Downs et al. [33]
247 using Microsoft Office Picture Manager. The method using Photoshop CS6 used mean RGB value
248 from the image histogram for each timed dose response piece and the unexposed control piece. Any
249 software that provides histogram image analysis can provide this information. The difference between
250 each mean RGB value was calculated and compared to the total change in RGB values observed
251 between the unexposed and fully saturated control pieces. This resulted in a ratio between 0 to 1. This
252 method is similar in technique to that devised by Downs et al. [33]. That technique was originally
253 used to measure ink fade but it applies equally to colour saturation. The method requires the image to
254 be converted to monochrome (or grey scale) images. In Microsoft Office Picture Manager this can be
255 achieved by changing colour settings of "Amount" and "Saturation" to zero. The image is then
256 processed by increasing contrast to 100, and then slowly decreasing brightness until the image turns
257 completely black. Alternatively, the brightness could also be increased until the image turns
258 completely white. The brightness level is then recorded. This is repeated for each image obtained per
259 timed dose and each control piece. The difference between the brightness of the timed dose response
260 and the unexposed control piece is then compared to the range of brightness between the unexposed
261 control piece and the fully saturated control piece. This results in a ratio between 0 and 1.

262 2.3 Response after development

263 The blueprint paper was exposed for a photogram image and developed by washing in water. Half of
264 the same sheet was exposed to further solar irradiance and then photographed for analysis to detect if
265 there was any further change.

266 2.4 The cyanotype process

267 The basic chemical experiment in the traditional wet lab of cyanotypes includes creation of
268 photograms (images made without a camera). Example items include film negatives, positive images
269 (black and white images printed on transparencies) and objects. Some of the manufacturing
270 companies provide other examples of possible photograms, showing that sunscreen will block UV
271 radiation and prevent the chemical reaction in the paper. The procedure for this latter experiment
272 recommends using glass slides or sheets of acrylic (provided in some kits made by the companies) to
273 apply sunscreen to cover the blueprint paper. Whilst this is an understandable idea, glass is an
274 unsuitable item to allow younger children to use in case of breakage and therefore has been avoided
275 by the authors. Additionally, both glass and acrylic absorb strongly in the UVB radiation spectrum
276 and are therefore blocking a portion of the UV spectrum that is explored. It is instead recommended
277 by the authors that polyethylene (plastic sheet protectors) is a suitable and cost effective replacement
278 for both these recommended items. Polyethylene has a high transmission across both the UV and
279 visible spectrum (ranging from 60% transmission at 280 nm to 80% transmission at 700 nm) as shown
280 in Figure 2 [32]. The plastic sheet protectors can be obtained in large quantities at any stationery store
281 for a reasonably low cost and are safe for younger children to use under supervision.

282

283 3.0 Results

284 3.1 Spectral Response

285 Figure 3 provides the spectral response as photographed images of the exposed and developed paper.
286 The paper used in this particular example is Paper 1, and is one of a set of two carried out on the same
287 day of testing. Figure 4 provides the image processed versions of the images shown in Figure 3 using
288 MultiSpec software to classify the pixels. The percentage count of blue pixels was tabulated per
289 wavelength, then normalised according to the maximum exposure count. For sheet 1, maximum blue
290 pixel count occurred at 300 nm and for sheet 2 maximum blue pixel count occurred at 330 nm.
291 Despite the variation between sheets of the same paper type there is a definite correlation between the
292 exposure wavelength and the sensitivity of the paper, with sensitivity decreasing as wavelength
293 increases. Early tests indicated that wavelengths above 430 nm may be a promoter of the chemical
294 reaction, though later tests that extend to 450 nm do not indicate any promoter effect of the chemical
295 reaction in the paper above 430 nm. It does show that violet light is able to produce the cyanotype
296 reaction, but with a lower effectiveness than for the UVB radiation. Figure 5 provides the data
297 obtained for Paper 1 type.

298 3.2 Dose response

299 The dose responses produced using the neutral density filters show increasing colour saturation with
300 increasing exposure time (Figure 6) with one layer used for the five minute exposure and two layers
301 used for the ten minute exposure. Also visible are “creases” from the neutral density filter, where the
302 filter was not stretched evenly. It was quite difficult to eliminate creases given the elasticity of the
303 filter. When correlated against pixel saturation and change in RGB mean or change in brightness
304 (Figures 7 a & b), the results are extremely similar for each method for both the five minute and ten
305 minute dose responses plotted against UVB irradiance. Both the five minute and ten minute dose
306 responses show a linear dose response. For the five minute dose response, the following lines of best
307 were noted: brightness $y = 9.4x + 0.9$ ($R^2 = 0.98$), RGB mean $y = 7.8x + 1.06$ ($R^2 = 0.96$),
308 ambient brightness $y = 361.3x + 36.9$ ($R^2 = 0.98$) and ambient RGB mean $y = 300.7x +$
309 43.3 ($R^2 = 0.96$). For the ten minute dose response, the following lines of best fit were noted:
310 brightness $y = 4.2x + 0.7$ ($R^2 = 0.97$), RGB mean $y = 4.3x + 0.6$ ($R^2 = 0.99$), ambient brightness
311 $y = 223x + 35.8$ ($R^2 = 0.97$) and ambient RGB mean $y = 228x + 31.2$ ($R^2 = 0.99$). It is
312 interesting to note that both the filtered UVB and ambient erythematous UV dose responses for the five
313 minute and ten minute sessions differ in exposure rates (Figure 7c). This is only in part due to the time
314 of day the dose responses were measured. The ten minute dose response was carried out later in the
315 afternoon when lower ambient exposures were experienced with the five minute dose response made
316 from 2.30 pm to 2.35 pm and the ten minute dose response made from 3.10 pm to 3.20 pm. Therefore
317 the ten minute exposure undergoes both less UV exposure due to lower ambient UV, with filtered UV
318 exposure extending the exposure time, resulting in a lower exposure rate. In addition, with the
319 saturation limitations of the blueprint paper and possibly batch or paper variation, it is not unexpected
320 that the exposure rates are different. Interestingly, it is observable here that the filtered UVB exposure
321 (from the IL1400 with neutral density filter) and the ambient erythematous exposure (from the Bentham
322 DTM300) are comparable for most of the dynamic response, with some variation occurring in the
323 measurements with deeper colour saturation.

324 3.3 Response after Development

325 There was no measurable dark reaction for the blueprint paper. Once the paper is washed, the salts are
326 removed completely from the paper and the reaction cannot continue. The image tested did not show
327 any change after development.

328 3.4 The cyanotype process

329 Figure 8 shows the result of a basic experiment using the blueprint paper, where an image printed in
330 black on overhead projector transparency sheets, has been superimposed on the blueprint paper.
331 Where the solar irradiance has been blocked from the blueprint paper, the reaction creating Prussian
332 Blue does not occur in these spaces. Therefore, the white/pale blue is a result of no reaction and dark

333 blue indicates the presence of Prussian blue and therefore the reaction. Images created without the use
334 of a camera are called a photogram. Therefore the image in Figure 8 is a photogram. Figure 9 is a
335 photogram made using an object of a joined coil of wire (similar to a slinky) instead of a transparency.
336 The angle of the image indicates the sun was at medium solar zenith angle (51 to 56.7° SZA), and not
337 only does the object block the reaction, but so do the shadowed areas. Where sunlight falls between
338 the coils, dark lines occur due to the reaction occurring. Therefore photograms can be made with
339 either two dimensional transparencies or three dimensional objects. Figure 10 shows the differences
340 that can occur in photograms made with overlying transparencies due to direct and indirect solar
341 irradiance. The left image has been produced under direct solar irradiance, and shows a relatively
342 clear image. The image on the right was produced on a cloudy day with diffuse solar irradiance. Parts
343 of the image appear blurred in comparison to the image on the left, which indicates that the diffuse
344 UV radiation does not produce as sharp an image as direct UV radiation. The image on the right
345 required several minutes of exposure on a cloudy day, whereas the image on the left required only two
346 minutes of exposure on a sunny day. Figure 11 shows a photogram of two circles, one dark and one
347 light. A plastic filter opaque to UV radiation but transparent to visible light (left circle) was used next
348 to a plastic filter that transmits both UV and visible radiation (right circle). The filter that was opaque
349 to UV radiation clearly shows a much lighter blue compared to the filter that transmits both UV
350 radiation and visible radiation. However, with longer exposure times, it is likely that saturation of the
351 blueprint paper would have eventually occurred due to visible radiation providing a reduced rate of
352 reaction to the cyanotype reaction. Figure 12 also confirms a basic experiment that some of the
353 companies who produce the blueprint paper, recommend as an observational experiment, in the use of
354 sunscreen as a UV blocker. In this version of the basic experiment, amount of application of
355 sunscreen is introduced to indicate protective capability. The active ingredient in each type of
356 sunscreen is listed in Table 2.

357

358 4.0 Discussion

359 The spectral response results are shown in Figures 3 to 5. The exposed areas are clearly defined due to
360 the film transparency aperture. However, it is apparent that the outer edges of the beam drop in
361 intensity despite the beam appearing to cover the entire film transparency aperture. This slight
362 variation in intensity is not an issue, as the pixel counting software counts all pixels that are classified
363 as “exposed” or “not exposed”. Another exposure at a different distance might provide a sharper
364 delineation to the output beam and is a possible future study to further clarify the spectral response.
365 Also, early tests indicated an uneven exposure to the paper, which revealed some alignment issues
366 with the irradiation monochromator that was then adjusted accordingly. To date, there has been no
367 spectral response investigated for the cyanotype chemical reaction that produces Prussian blue. The

368 method used in this study is a completely new method to investigate influence of UV radiation
369 wavelength on the cyanotype chemical reaction that produces Prussian blue, with no information
370 provided in the literature reviewed. Given that many UV radiation induced action spectra normally
371 have strong sensitivity in the shorter UVB wavelengths, it is interesting to observe that the longer
372 UVB range and shorter UVA range had the most sensitivity in producing the product Prussian blue,
373 with a skewed bell shaped curve. The pixel counting software (Figure 4 shows the data obtained using
374 MultiSpec for Windows) also indicates that the effect of wavelengths greater than 420 nm are not
375 effective at producing Prussian blue. Young, Freedman & Ford [34] stipulate that the wavelength
376 range of 400 nm to 450 nm is classified as violet coloured irradiance, and wavelength from 450 nm
377 upwards is classified as blue wavelengths. Therefore, it appears ultraviolet and violet classified
378 wavelengths are the only effective wavelengths to produce the chemical reaction, rather than the
379 previously assumed range of ultraviolet radiation to blue radiation.

380 Additionally, it was found that variation in this spectral response varied with Paper type. There was
381 variation also observed with different batches of the same Paper type, and to a lesser extent, the
382 separate sheets within a batch of the same Paper type. This suggests that the production methods of
383 the different companies, and even within manufacturing processes, result in variation in the chemical
384 density of reagents present. This would account for the variation in exposed pixels counted in some of
385 the preliminary test results. An expression of the uncertainty of the spectral response cannot be
386 calculated given that only three spectral response data measurements for each point in the spectrum
387 have been obtained. This is not enough data to provide confidence in statistical analysis until further
388 repeated measurements can be made. Variations between batch types and paper type will also
389 introduce further uncertainty that will need to be investigated.

390 The five minute and ten minute dose response tests show similarity (Figure 6) in depth of colour
391 saturation. A comparison of the RGB mean in each dose response shows that the saturation level of
392 each exposed piece (as indicated in Figure 7 (a & b)) is approximately the same for each
393 corresponding time, which also means dynamic response is limited to short time periods unless
394 alternative neutral density filters are used. In other words, they appear the same visually. For example,
395 the 7 minute exposure corresponds to 3.5 minute exposure – which is the 8th exposed piece from the
396 left in Figure 6. The colour range indicated by the unexposed to the fully exposed shows that only a
397 limited dynamic range may be supported by the blueprint paper. The maximum variance in mean
398 RGB between saturation levels at each corresponding colours is 10%. This suggests that the neutral
399 density filter, despite the average difference of transmission varying by a factor of four, indicates only
400 a factor of two difference between layers with exposure time. One neutral density filter layer used
401 with half minute intervals corresponds with a double neutral density filter layer used with minute
402 intervals, although exact double UV exposure is not observed in Figure 7b or Figure 7c. In fact,
403 erythemal exposure is actually lower in this data set given that the dose response was carried out later

404 in the afternoon compared to the five minute dose response (Figure 7a). Figure 7c indicates that the
405 differing exposure with differing neutral density filters produce different dose responses. Ideally these
406 dose responses should be carried out over the noon period to reduce significant variation. However, it
407 can be beneficial to use this variation to enforce the conceptual understanding for students that UV
408 exposure varies significantly over the day. It is indicative that using either method of image analysis
409 (brightness change or RGB mean change) produces similar results and thus either method is suitable
410 for a basic analysis of the dynamic response. This can then be used as a method of approximating UV
411 exposure in short periods of time. If equipment is not available for use as indicated in the
412 methodology, Downs et al. [23] have shown that an Edison UV checker can be used as an inexpensive
413 means to measure ambient UV exposure in order to carry out a dose response calculation as shown in
414 Figures 7 (a) & (b). This affordable instrument has previously been used successfully in other
415 dosimetry experiments [33, 35]. It was also interesting to observe the creases produced in some of the
416 images from the addition of the neutral density filter. By taking non-creased segments of an image
417 that had a visible crease, the mean response from the histogram of those images did not change, nor
418 did the brightness. Therefore “creases” from the neutral density filter did not affect the production of
419 the dose response. However, it is advised that the filter should always be fixed as flat as possible.

420 Many of the recommended experiments from the paper manufacturers confirm that which has been
421 done before. However this study shows that UV radiation is the most effective initiator of the
422 cyanotype reaction. A further potential experiment that might be explored for younger children is the
423 concept of translating three dimensional objects into two dimensional images. This might simply
424 involve younger students working out how to make specific patterns using shade from three
425 dimensional objects. This may provide students a connection between UV exposure and shade (shade
426 reduces exposure). However this should be used cautiously if the intention is to demonstrate that
427 shade does not block all UV exposure (as shown in Figure 10) and even in shaded situations relatively
428 sharp images can be produced. In this Figure it is also interesting to note that blurring occurs within
429 the image (see highlighted areas). This blurring is not due to the layer of image transparency moving,
430 and could be attributed to the diffuse nature of the UV exposure, which again may be a suitable
431 variation in an investigation to explore the properties of UV radiation exposure. It may be suitable to
432 investigate the differences between photograms made in direct sunlight and indirect sunlight for
433 younger students, so as to introduce students to duration of exposure time and how the exposure is
434 obtained. In moving onto exploring the difference between ultraviolet and visible radiation, the filters
435 used in Figure 11 are inexpensive to obtain (originally obtained from the same supplier as Paper 1)
436 and can then be included in experiments to stimulate discussion on whether solar ultraviolet radiation
437 can be present inside buildings as opposed to outside.

438 The sunscreen test is recommended for public outreach, where a number of sunscreens might be
439 compared against one another for effectiveness, mainly for investigation of ease of application and

440 amount of application. Using the modified method outlined in this study, this experiment has been
441 successfully used by children aged five and up to show the effectiveness in application of sunscreen
442 (level of thickness). From Figure 12 we can see that of the three types tested, Sunscreen number 3
443 appears to show the best spread-ability and coverage for layers of thin to thick, but sunscreen 2
444 apparently shows the maximum blocking ability for its thickest layer. An experiment such as this is a
445 good reminder to students and to the public that generous application of sunscreen is more effective
446 than light application of sunscreen. Studies show that sunscreen is not regularly applied at the
447 recommended amounts [36, 37]. The Cancer Council of Australia recommends a minimum of one
448 half to one teaspoon of sunscreen applied per limb. This recommendation is based on the
449 internationally accepted amount of sunscreen application at 2 mg/cm^2 [36, 37] and is equivalent to an
450 average of nine teaspoons of sunscreen applied on an adult [38]. All the sunscreens used were sun
451 protection factor (SPF) 30+ with different active ingredients (see Table 2). At this stage this style of
452 basic test would be unable to provide analysis between different active ingredients given it can be
453 difficult to apply the sunscreen evenly to a slippery surface. It is also unlikely that tests to look at
454 different SPF would provide useful information, given that the difference between SPF 30 and SPF 50
455 protection is about 3%, with a non-linear protection scale. However, future tests could easily include
456 investigating application methods (spray versus roll on versus application by hand) which may
457 provide further extension to these studies.

458 Of all the characterisation tests carried out in this study, the spectral sensitivity response test is the
459 least likely to be effective in public demonstrations given the equipment and extensive analysis
460 techniques required. However, prior development of a sheet of spectral sensitivity such as those in
461 Figure 3, could be made to use as a visual aid in any public outreach. The dose response technique, is
462 easily demonstrated in a real time experiment, and visual comparison of results could be estimated if
463 the demonstration incorporated factors such as the exposure of paper to UV in a shaded environment,
464 and by comparing it to the dynamic response calibration to determine how much UV exposure is
465 obtained in a short time in a shaded environment. Measurements made at noon even with a neutral
466 density filter may require shorter time periods to ensure saturation is not achieved too soon throughout
467 the experiment. The analysis can then be carried out within an hour of the initial exposures, or even
468 estimated when observed in real time during the blue to white fade observed as the paper is exposed.
469 The more straightforward experiments outlined last in this study are the most likely to be able to
470 capture interest at the beginning of any outreach plan. Suggested further studies include investigation
471 of the effectiveness of application of spray on sun screen, including both the alcohol based sprays
472 compared to pump action cream sprays and standard cream application.

473 Through this investigation, the authors have found a direct link with wavelength and the reaction that
474 produces Prussian blue. This is a significant step in the understanding of the cyanotype reaction that
475 deserves further attention to shed further light on nature of this chemical process.

476

477 Acknowledgements

478 The authors would like to thank Laboratory Officer Kim Larsen for his assistance and consultation
479 with this study.

480 References

- 481
- 482 1. Smith, B. J., Ferguson, C., McKenzie, J., Bauman, A., and Vita, P., Impacts from repeated mass
483 media campaigns to promote sun protection in Australia. *Health Promotion International*,
484 2002. **17**(1): p. 51-60.
 - 485 2. McCarthy, W., The Australian Experience in Sun Protection and Screening for Melanoma.
486 *Journal of Surgical Oncology*, 2004. **86**: p. 236-245.
 - 487 3. Armstrong, B. K. and Kricger, A., The epidemiology of UV induced skin cancer. *Journal of*
488 *Photochemistry and Photobiology B: Biology*, 2001. **63**: p. 8-18.
 - 489 4. Godar, D. E., UV Doses Worldwide. *Photochemistry and Photobiology*, 2005. **81**: p. 736-749.
 - 490 5. de Gruijl, F., Skin cancer and solar UV radiation. *European Journal of Cancer*, 1999. **35**(14): p.
491 2003-2009.
 - 492 6. Lemus-Deschamps, L. and Makin, J. K., Fifty years of changes in UV Index and implications for
493 skin cancer in Australia. *International Journal of Biometeorology*, 2012. **56**: p. 727-735.
 - 494 7. Mckenzie, R., Aucamp, P., Bais, A., Bjorn, L., Ilyas, M., and Madronich, S., Ozone depletion
495 and climate change: impacts on UV radiation. *Photochemical and Photobiological Sciences*,
496 2011. **10**: p. 182-198.
 - 497 8. Lucas, R. M., McMichael, A. J., Armstrong, B. K., and Smith, W. T., Estimating the global
498 disease burden due to ultraviolet radiation exposure. *International Journal of Epidemiology*,
499 2008. **37**: p. 654-667.
 - 500 9. English, D., Armstrong, B. K., Kricger, A., and Fleming, C., Sunlight and Cancer. *Cancer Causes*
501 *and Control*, 1997. **8**: p. 271-283.
 - 502 10. Carter, O. B. and Donovan, R. J., Public (Mis)understanding of the UV Index. *Journal of Health*
503 *Communication*, 2007. **12**: p. 41-52.
 - 504 11. Stengel, F. M. and Fernandez, J. F., Education and behavioral change for sun protection.
505 *Journal of Cosmetic Dermatology*, 2005. **4**: p. 83-88.
 - 506 12. Stanton, W. R., Janda, M., Baade, P. D., and Anderson, P., Primary prevention of skin cancer:
507 a review of sun protection in Australia and internationally. *Health Promotion International*,
508 2004. **19**(3): p. 369-378.
 - 509 13. Saraiya, M., Glanz, K., Briss, P. A., Nichols, P., White, C., Das, D., Smith, S. J., Tannor, B.,
510 Hutchinson, A. B., Wilson, K. M., Gandhi, N., Lee, N. C., Rimer, B., Coates, R. C., Kerner, J. F.,
511 Hiatt, R. A., Buffler, P., and Rochester, P., Interventions to prevent skin cancer by reducing
512 exposure to ultraviolet radiation: A systematic review. *American Journal of Preventative*
513 *Medicine*, 2004. **27**(5): p. 422-466.
 - 514 14. Hill, D., White, V., Marks, R., Theobald, T., Borland, R., and Roy, C., Melanoma prevention:
515 behavioral and nonbehavioral factors in sunburn among Australian urban population.
516 *Preventative Medicine*, 1992. **21**(5): p. 654-669.
 - 517 15. Milon, A., Sottas, P.-E., Bulliard, J.-L., and Vernez, D., Effective exposure to solar UV in
518 building workers: influence of local and individual factors. *Journal of Exposure Science and*
519 *Environmental Epidemiology*, 2007. **17**: p. 58-68.
 - 520 16. Honigsmann, H., Erythema and pigmentation. *Photodermatology, Photoimmunology &*
521 *Photomedicine*, 2002. **18**: p. 75-81.
 - 522 17. Sliney, D., Epidemiological studies of sunlight and cataract: the critical factor of ultraviolet
523 exposure geometry. *Ophthalmic Epidemiology*, 1994. **1**(2): p. 107-119.
 - 524 18. Hershel, J. F. W., On the action of rays of the solar spectrum on vegetable colours, and on
525 some new photographic processes. *Philosophical Transactions of the Royal Society of*
526 *London*, 1842. **132**: p. 181-214.
 - 527 19. Ware, M., *Cyanotype: The history, science and art of photographic printing in Prussian blue*.
528 1999, Bradford, England: National Museum of Photography, Film & Television.
 - 529 20. Davidson, D., The Formulation of Prussian Blue. *Journal of Chemical Education*, 1937. **14**(6):
530 p. 277-281.

- 531 21. Ware, M., The molecular basis of blueprinting, in *Cyanotype: The history, science and art of*
532 *photographic printing in Prussian blue*. 1999, National Museum of Photography, Film &
533 Television: Bradford, Englad. p. 39-47.
- 534 22. Lawrence, G. D. and Fishelson, S., UV Catalysis, Cyanotype Photography and Sunscreens.
535 *Journal of Chemical Education*, 1999. **76**(9): p. 1199-1200.
- 536 23. Downs, N., Larsen, K., Parisi, A., Schouten, P., and Brennan, C., A practical science
537 investigation for middle school students: Designing a simple cost effective chemical solar
538 radiation dosimeter. *Teaching Science*, 2012. **58**(1): p. 48-51.
- 539 24. Lawrence, G. D. and Fishelson, S., Blueprint Photography by the Cyanotype Process. *Journal*
540 *of Chemical Education*, 1999. **76**(9): p. 1216A-1216B.
- 541 25. Price, S. F., Schuette, M. L., and Tassie, E., Measuring incident light graph clusters using
542 photosensitive paper and image analysis. *Journal of the American Society for Horticultural*
543 *Science*, 1995. **120**(2): p. 235-240.
- 544 26. Friend, D., A simple method of measuring integrated light values in the field. *Ecology*, 1961.
545 **42**(3): p. 577-580.
- 546 27. CIE, A reference action spectrum for ultraviolet induced erythema in human skin. *CIE*, 1987.
547 **6**: p. 17-22.
- 548 28. Mckenzie, R. and Madronich, S., Ultraviolet, Surface, in *Encyclopedia of Atmospheric*
549 *Sciences*, R.H. James, Editor. 2003, Academic Press: Oxford. p. 2474-2480.
- 550 29. Diffey, B., Source and measurement of ultraviolet radiation. *Methods*, 2002. **28**(1): p. 4-13.
- 551 30. Stamnes, K., Ultraviolet radiation, in *Encyclopedia of Atmospheric Sciences*, R.H. James,
552 Editor. 2003, Academic Press: Oxford. p. 2467-2473.
- 553 31. Downs, N., Parisi, A., Turner, J., and Turnbull, D., Modelling ultraviolet exposures in a school
554 environment. *Photochemical and Photobiological Sciences*, 2008. **7**(6): p. 700-710.
- 555 32. Turner, J. and Parisi, A. V., Simple experiments to visualise and simulate the biological impact
556 of ultraviolet radiation, in *2014 NIWA UV Workshop*, R. Mckenzie, Editor 2014: Auckland,
557 New Zealand.
- 558 33. Downs, N., Turner, J., Parisi, A., and Spence, J., Pen ink as an ultraviolet dosimeter. *Teaching*
559 *Science*, 2008. **54**(4): p. 41-44.
- 560 34. Young, H. D., Freedman, R. A., and Ford, L., *Sears and Zemansky's University Physics with*
561 *Modern Physics*. 2008, San Francisco, USA: Pearson Addison-Wesley.
- 562 35. Downs, N., Parisi, A., Powell, S., Turner, J., and Brennan, C., Extensions in pen ink dosimetry:
563 Ultraviolet calibration applications for primary and secondary schools. *Teaching Science*,
564 2010. **56**(1): p. 51-56.
- 565 36. Bauer, U., O'Brien, D. S., and Kimlin, M. G., A new method to quantify the application
566 thickness of sunscreen on skin *Photochemistry and Photobiology*, 2010. **86**: p. 1397-1403.
- 567 37. Petersen, B. and Wulf, H. C., Application of sunscreen - theory and reality.
568 *Photodermatology, Photoimmunology & Photomedicine*, 2014. **30**: p. 96-101.
- 569 38. Isedah, P., Osterwalder, U., and Lim, H. W., Teaspoon rule revisited: proper amount of
570 sunscreen application. *Photodermatology, Photoimmunology & Photomedicine*, 2012. **29**(1):
571 p. 55-56.

572

573

574 Table 1- Information on the types of blueprint paper.

Paper No.	Company	Blueprint paper name	Website	Australian Distributor
1	NaturePrint Paper	Nature Print Paper	www.natureprintpaper.com	Haines Educational
2	Lawrence Hall of Science, University of California, Berkely	Sunprint Paper	www.sunprints.org	Prof Bunsen Science
3	TEDCO Toys	Sun Art Paper	www.tedcotoys.com	Not available

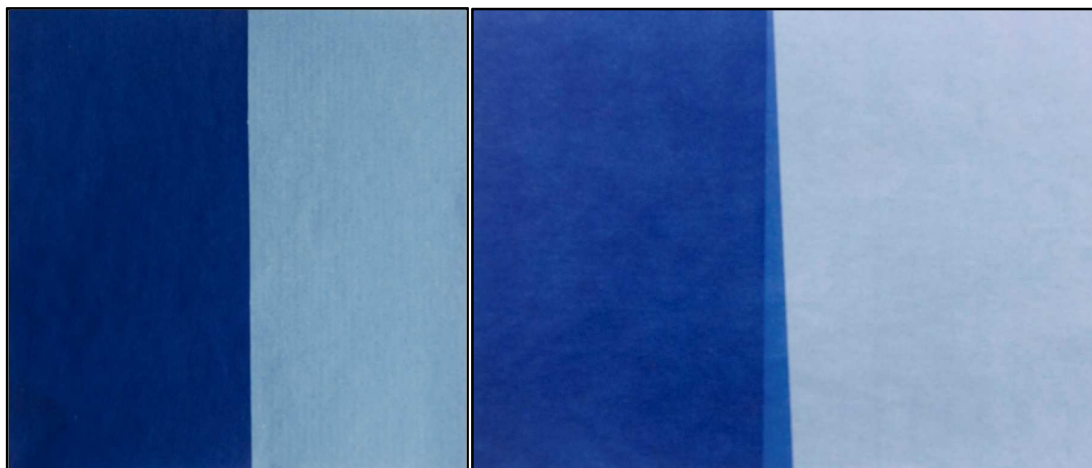
575

576 Table 2 - Information on the active ingredients in the sunscreens.

Sunscreen Number	Active ingredients	SPF	Spectrum protection claim
1	Homosalate 5% Octisalate 5% Oxybenzone 5% Avobenzone 3% Octocrylene 2.7%	30+	Not available (sample only)
2	Octyl methoxycinnamate 7.5% Octocrylene 4.0% Zinc oxide 4.75% Titanium dioxide 1.5%	30+	Broadband
3	Zinc oxide 18%	30+	High UVB+UVA

577

578



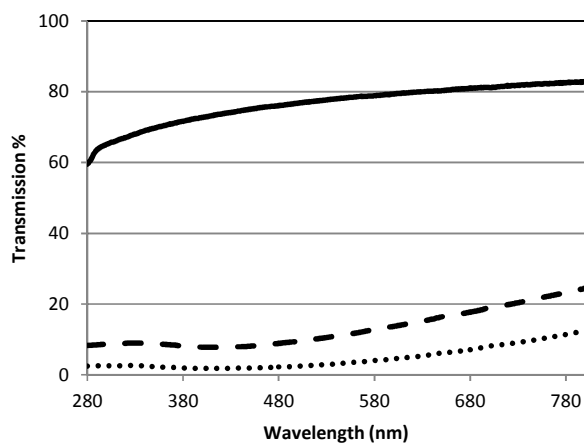
579

580 Figure 1 – Example references sheet of “no exposure” (light blue) to “saturated exposure” (dark blue).

581 Note that paper type shows different levels of saturation where Paper 2 (left) has darker saturation

582 than Paper 1 (right).

583

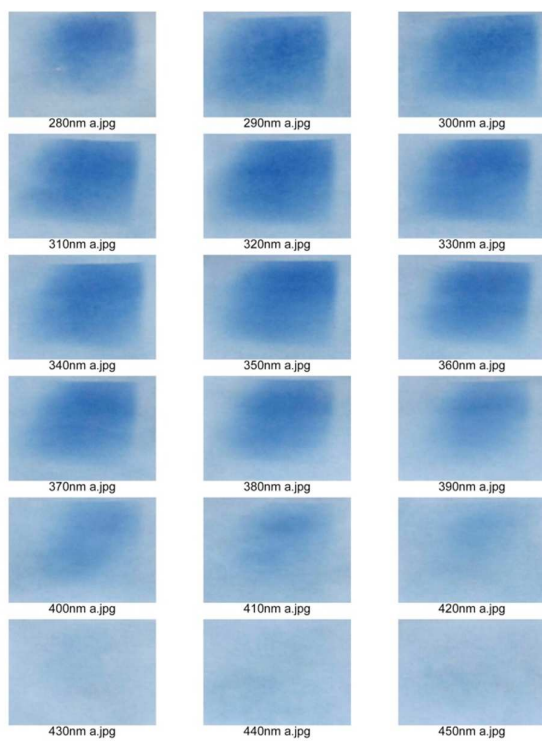


584

585 Figure 2 – Transmission of polyethylene (unbroken line), single layer of neutral density filter (wide

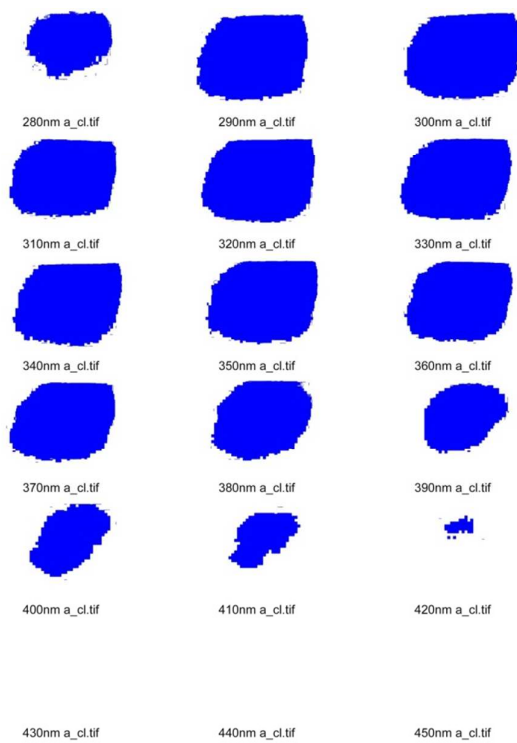
586 broken line) and double layer of neutral density filter (thin broken line). Figure reproduced with

587 permission [32].



588

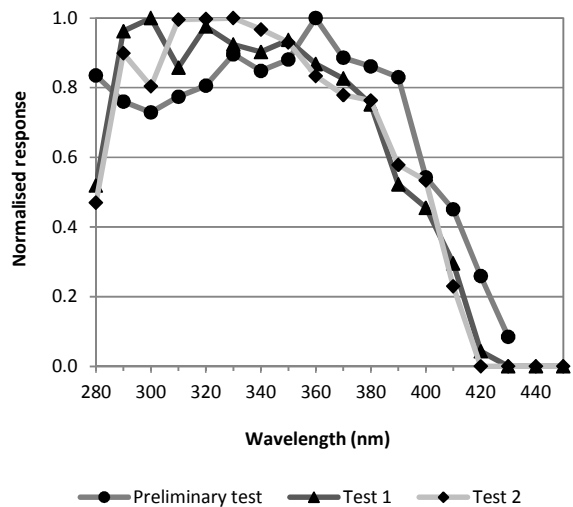
589 Figure 3 - Exposure to 2000 J/m² per wavelength at 16.4 cm from outside of source.



590

591 Figure 4 - Pixel count corresponding images to the spectral test, using MultiSpec for windows
592 software.

593



594

595 Figure 5 – Spectral response of blueprint paper using the pixel counting analysis according to
596 different sheets used from one paper type (Paper 1) exposed at each wavelength to 2000 J/m².

597

598

599



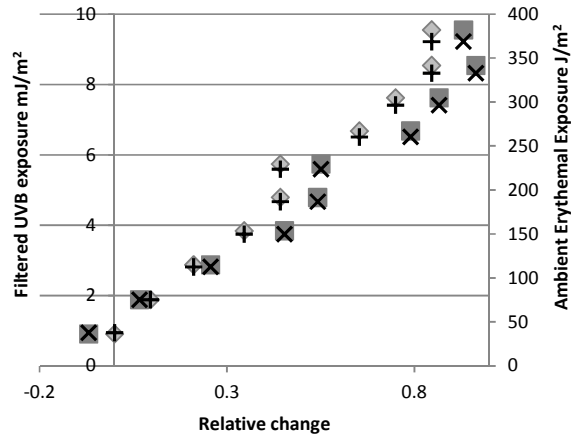
600

601

602 Figure 6 - Dose response using a single layer of neutral density filter for a five minute period (top)
603 and a double layer of neutral density filter for a ten minute period (bottom). Each dose response set
604 has an unexposed control piece (extreme left) and a fully exposed (saturated) control piece (extreme
605 right). Each piece is placed in sequential order of dose exposure time.

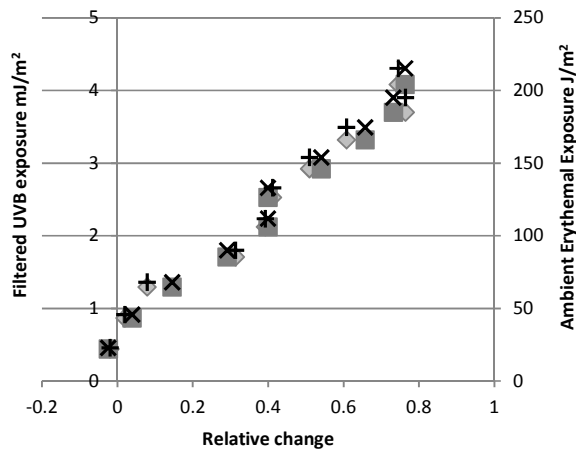
606

607



608

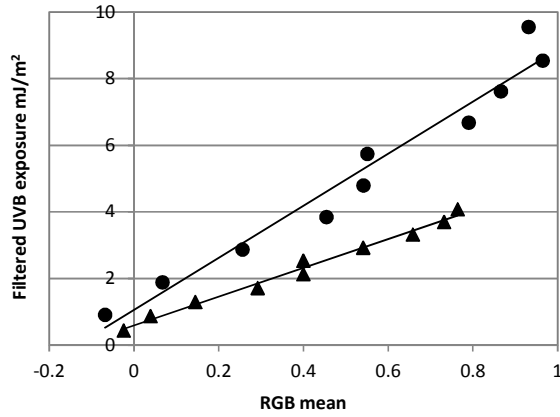
609 Figure 7(a) – Dose response for 5 minute series (with double neutral density layer) for brightness
 610 (diamond) and RGB mean (square). The ambient measurements for each method is included to show
 611 calibration is possible: ambient using brightness method (+) and ambient using RGB method (×).



612

613 Figure 7 (b) – Dose response for 10 minute series (with double neutral density layer) for brightness
 614 (diamond) and RGB mean (square). The ambient measurements for each method is included to show
 615 calibration is possible: ambient using brightness method (+) and ambient using RGB method (×).

616



617

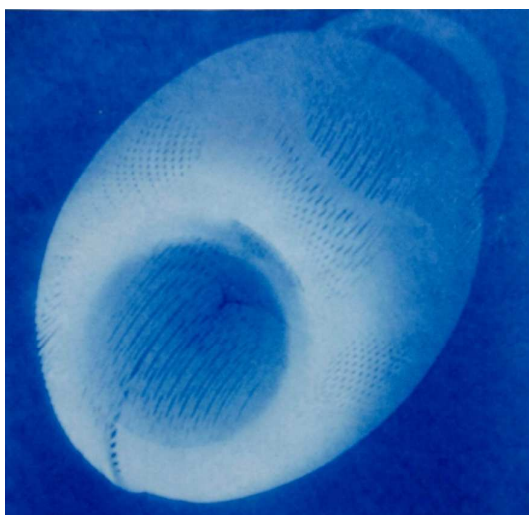
618 Figure 7 (c) – Comparison between dose response using relative change in RGB mean for the 5
619 minute series (one layer of neutral density filter) $y = 7.8x + 1.1$; $R^2 = 0.96$ and 10 minute series
620 (two layers of neutral density filter) $y = 4.3x + 0.6$; $R^2 = 0.99$.

621



622

623 Figure 8 - Photogram created using an image on a transparent sheet



624

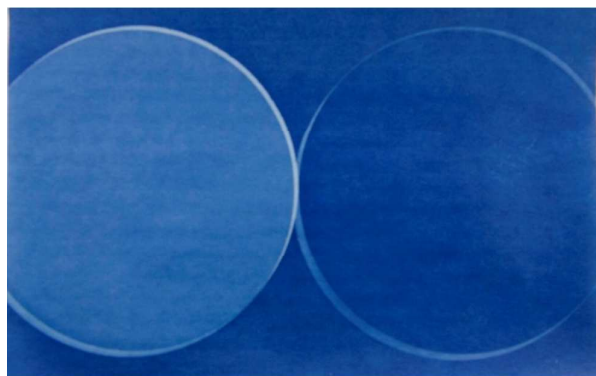
625 Figure 9 - Photogram using an object (connected slinky spring) with sun at a medium SZA. Shadows
626 and light are recorded on the image.

627



628

629 Figure 10 - Photograms using transparent prints. The image on the left was produced in direct
 630 sunlight in less than five minutes. Most of the image is relatively clear. The image on the right was
 631 produced under shade with diffuse radiation and took five to ten minutes to produce. Parts of the
 632 image are blurred (see highlighted areas); however this is not due to image movement.



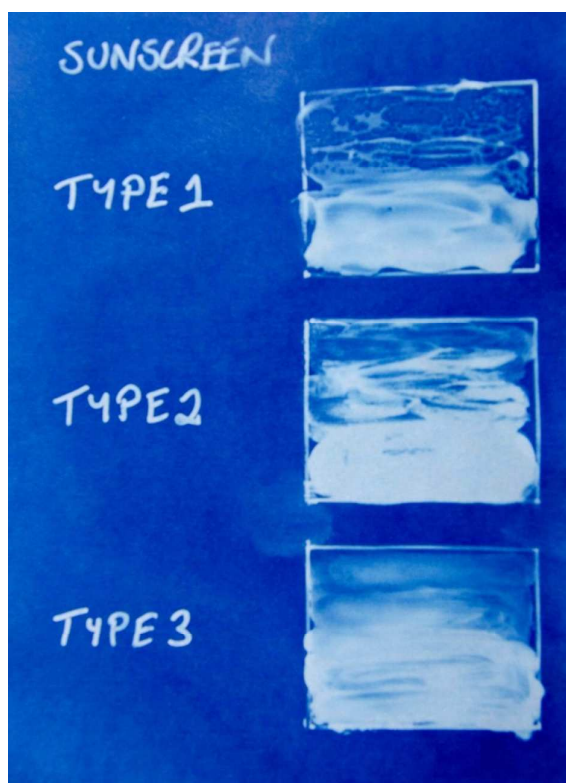
633

634 Figure 11 - Simple plastic UV filters shows that UV is part of the main reactive energy source to
 635 produce the reaction. The circle filter on the left was opaque to UV radiation whilst the one on the
 636 right was transparent to UV. However, long exposure with the opaque filter would have eventuated in
 637 a reaction due to the visible sensitivity.

638

639

640



641

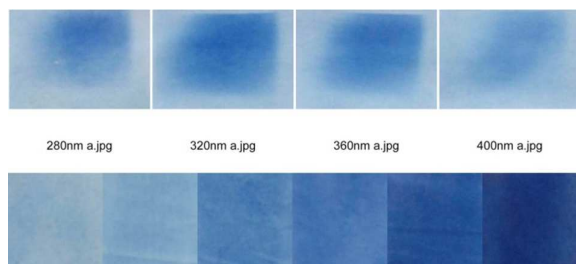
642 Figure 12 - Basic sunscreen tests comparing sunscreen type can be carried out. Three different
643 sunscreens were tested at varying thicknesses (thinnest layer at the top of each box graduated in
644 increasing thickness to the bottom of the box).

645

646

647

648



The cyanotype process is characterised via dynamic and spectral response in an educational toy (blue print paper) that can be used to provide outreach activities for UV exposure applications.